Effect of Shear Rate on Structural, Mechanical, and Barrier Properties of Chitosan/Montmorillonite Nanocomposite Film

Seung In Hong,[1] Jin Hwan Lee,[2] Ho Jae Bae,[3] Song Yi Koo,[4] Hyun Soo Lee,[5] Jae Hoon Choi,[5] Dong Hyun Kim,[6] Seok-Hoon Park,[1] Hyun Jin Park[1,3]

[1]*College of Life Sciences and Biotechnology, Korea University, 5ga Anam-Dong, Sungbuk-Ku, Seoul 136-701, Republic of Korea*
[2]*CJ Cheil Jedang Food F&D Package Development Center, CJ CjeilJedang Corporation, Hankyung Bldg. 441, Jungnim-dong, Jung-gu, Seoul 100-791, Republic of Korea*
[3]*Department of Packaging Science, Clemson University, Clemson, South Carolina 29634-0320*
[4]*KIST Gangneung Institute, Gangneung Techno valley, 290 Daejeon-dong, Gangneung, Gangwon-do 210-340, Republic of Korea*
[5]*Research Development Department, LOTTE ALUMINIUM Co., LTD., 1005 Doksan-dong, Geumcheon-gu, Seoul 153-010, Republic of Korea*
[6]*Korea Institue of Industrial Technology, Sangrok-gu, Ansan-si, Gyeonggi-do 426-791, Republic of Korea*

Received 4 May 2009; accepted 8 November 2009
DOI 10.1002/app.31767
Published online 13 September 2010 in Wiley Online Library (wileyonlinelibrary.com).

ABSTRACT: The dispersion of MMT-Na^+ (montmorillonite) layers in a chitosan polymer matrix, using the homogenization, was performed. The effect of shear rate was characterized on the mechanical, barrier, and structural properties of nanocomposites. Elongation at break (EAB) was unaffected by shear rate, which decreased after homogenization, increased above 13,000 rpm, however, tensile strength (TS) dramatically increased up to 59 MPa at 16,000 rpm. Water vapor permeability (WVP) and oxygen permeability (OP) of the homogenized nanocomposite decreased more than that of untreated nanocomposite and OP was not significantly changed above 16,000 rpm of shear rate. XRD result and TEM images indicated that three types of tactoids, exfoliation, and intercalation were generated and the largest distance of 18.87 Å between MMT-Na^+ layers was produced at 16,000 rpm. The results indicate that homogenization was a beneficial method for effectively dispersing MMT-Na^+ layers in a chitosan polymer matrix and that a shear rate of 16,000 rpm was the effective condition. © 2010 Wiley Periodicals, Inc. J Appl Polym Sci 119: 2742–2749, 2011

Key words: nanocomposites; clay; barrier; mechanical properties; morphology

INTRODUCTION

The incorporation of a small amount of clay particles (2–6% by weight) into a polymeric matrix has received considerable research attention. The polymer nanocomposites exhibit remarkable improvement in mechanical, thermal, barrier, and electrochemical properties when compared with the pure polymer.[1–5]

Montmorillonite (MMT) is the most widely used as cationic clay of the smectite group in the generation of polymer nanocomposites. It consists of the stacking of layers of the 2 : 1 type clays (about 1.0 nm thick), which a sheet of the $M(O,OH)_6$ octahedra (where M = Al^{3+}, Mg^{2+}, Fe^{3+}, or Fe^{2+}) is sandwiched between two sheets of the Si(O,OH) tetrahedral. The negative charges are generated by isomorphous substitution occurred in the octahedral sheets (Mg^{2+} for part of the Al^{3+}) and they are counterbalanced by some cations, such as Na^+ in the gallery.[6,7] Because of the presence of cations adsorbed on the silicate layer, the cations inside the gallery can be easily exchanged by other cations. The technologies have implications in humidity sensors, electrochemical sensors, and in sewage disposal, such as the adsorption of metals and dyes.[8–11]

When nanoclay is mixed with a polymer, three types of nanocomposites (tactoids, intercalation, and exfoliation) are obtained, depending on the arrangement of the clay. In the case of tactoids (flocculation), the layers of clay particle do not separate due to hydroxylated edge–edge interactions and complete clay particles are dispersed within the polymer matrix. Intercalation and exfoliation are two ideal nanoscale composites. Intercalation occurs when polymer chains are intercalated into

Correspondence to: S.-H. Park (mickey06@korea.ac.kr) or H. J. Park (hjpark@korea.ac.kr).

Seung In Hong and Jin Hwan Lee equally contributed to this work as co-first authors and Seok-Hoon Park and Hyun Jin Park equally contributed as co-corresponding authors.

Contract grant sponsor: Lotte Aluminium Co. Ltd. (under the project "Development of Eco-packaging Solution Technology"); contract grant number: 100031979.

the layers of the clay, thus expanding the interlayer spacing and forming a well-ordered multilayer structure. In exfoliation (delamination), the layers of the clay are completely separated and homogeneously dispersed in the polymer matrix. The various properties (i.e., physical and mechanical properties) of nanocomposites changed depending on the structure of the clay layers.[5,12,13]

Chitosan (CS) is useful for healing, artificial skin, food preservation, cosmetics, and wastewater treatment due to its nontoxic nature, antimicrobial activity, and good compatibility with living tissue.[14,15] However, it has a disadvantage for the application in the high-humid condition because of its hydrophilic nature and its poor mechanical properties. Also, its thermal stability, hardness, and gas barrier property are not adequate enough to meet the wide ranges of potential applications. Numerous studies have been performed to find ways to enhance the mechanical properties of chitosan film using nanoclay and to elucidate the structural property of CS-clay nanocomposites.[5,13,16] However, few methods of improving the barrier property of CS/clay nanocomposites have been identified.

It is important to control the state of dispersion/distribution of clay layers within the molten polymer during the processing step. The considerable processing factors affecting these properties are shear rate (rpm), shear strain (time for a given rpm), and shear stress.[17] The perfect superimposed flat platelets will interact via van der Waals forces, which are larger than the energy of covalent carbon–carbon bond (84 kcal/mol), and occur at short distances. Intercalation not only facilitates the diffusion of polymeric chains inside the clay galleries but most importantly lowers the energy of adhesion to below that of a covalent carbon–carbon bond. Ion exchange helps to decrease the potential energy between layers, and the polymer diffusion into clay layers can be improved by this processing method.[17]

Therefore, in this study, the barrier property and the mechanical property were determined using CS/MMT nanocomposite. The method used for the dispersion of MMT-Na^+ layers in chitosan polymer matrix was as described by Bousmina.[17] This method lowers the interaction energy between MMT-Na^+ layers because of ion exchange that takes place between the Na^+ of MMT and the $-NH_3^+$ in the chitosan. Also, the effect of homogenization relative to shear rate was determined to facilitate the effective diffusion of chitosan polymer chains into MMT-Na^+ during the preparation of the nanocomposite.

MATERIALS AND METHODS

Materials

Chitosan (CS) was purchased from Samsung Chitopia Co. (South Korea), had a degree of deacetylation of 88.8%, and viscosity of 150 cps. The pristine montmorillonite (MMT-Na^+), with a cationic exchange capacity (CEC) of 115 mequiv/100 g, was supplied by Kunimine Industries Co., Ltd. (Japan), Rhodamine B was purchased from Aldrich Co.

Preparation of CS/MMT nanocomposite films

Chitosan/montmorillonite (CS/MMT) nanocomposite films were prepared using a casting technique. A chitosan aqueous solution was prepared by dissolving 4 g of chitosan powder into 250 mL of distilled water containing 1% (v/v) acetic acid. This chitosan solution was mixed with a mechanical stirrer until fully dissolved. Next, 40% (by weight) of glycerol was added to the chitosan solution and then glycerol was homogeneously dispersed by vigorous stirring. All samples included glycerol as a plasticizer because the chitosan film without glycerol was very brittle. Suspensions, containing varying amounts of MMT-Na^+ (from 1 to 11% by weight), were prepared in 1% (v/v) acetic acid solution. These MMT-Na^+ suspensions were then treated in an ultrasonic bath for 1 h to expand the gap of MMT-Na^+ layers. After the ultrasonic treatment, the chitosan solution and MMT-Na^+ suspension were mixed using a magnetic stirrer for 1 h. To obtain CS/MMT nanocomposite films, CS/MMT solutions were poured onto Teflon-coated glass plates and dried at room temperature for 48 h. These samples were used to measure the efficiency according to MMT-Na^+ contents.

Figure 1 shows the effect of MMT-Na^+ on oxygen transmission depending on the arrangement of the MMT-Na^+ in the chitosan membrane. The homogenization was performed after mixing the MMT-Na^+ suspension with the chitosan solution (using a magnetic stirrer) to effectively intercalate chitosan polymer chains into layers of MMT-Na^+. Finally, the mixture was homogenized in an ultrasonic bath for 25 min with different shear rates (0–22,000 rpm),

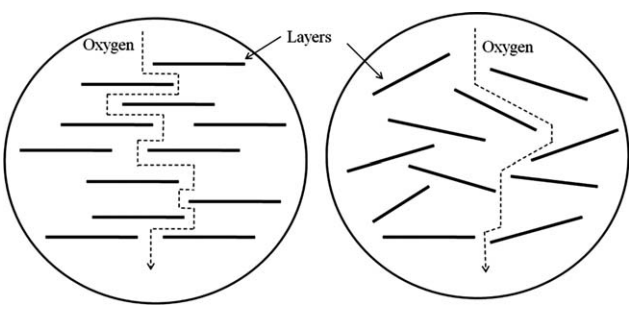

Figure 1 The scheme of oxygen transmission pathway depending on the arrangement of clay in chitosan membrane.

and the nanocomposite film was made using the casting technique.

Mechanical properties

An Instron Universal Testing Instrument Model No. 5566 (Instron) was used to measure tensile strength (TS) and elongation at break (EAB). Specimen size was 2.54 cm × 10 cm and film thickness was measured using a digital micrometer (ID-C112, Mitutoyo Corp., Japan) at five random positions on each film specimen to an accuracy of ±1 μm. All specimens were conditioned at 25°C, and an RH of 50% for 24 h. The tests were carried out at 23°C and an RH of 50%. Each determination was taken from an average of five specimens. Testing speed was 100 mm/min and the load cell was 500N. TS values were calculated by dividing the maximum peak load by the cross-sectional area. EAB was calculated by dividing the elongation at the moment of rupture by the initial length of specimen and multiplying by 100.

Oxygen permeability

Oxygen permeability (OP) was measured by using a MOCON OX-TRAN® Model 2/60 (MOCON Inc.). Testing was performed at 30°C under an RH of 50% (ASTM D 3985-05). The oxygen transmission rate (OTR) was obtained in cc O_2/m^2 day and converted into SI units. Measurements were taken three times and the average value was calculated. Multiplying these values by film thickness provided oxygen diffusion coefficients and pressure. Film thickness was measured immediately using a digital micrometer before film samples were put on the testing cell. All specimens were conditioned at 25°C, and an RH of 50% for 24 h.

Water vapor permeability

The water vapor permeability (WVP) of films was measured at 25°C using the ASTM (E96-80) procedure which was modified for the vapor pressure at the film underside. Sample sizes were 10 cm × 10 cm and they were equilibrated at an RH of 50% for 48 h. Films were then sealed to cups containing distilled water and placed in an air-circulated chamber equilibrated at 25°C and an RH of 50%. Film thickness was measured by digital micrometer. The steady-state water vapor flow was reached within 2 h for all films. Slopes were calculated by linear regression and correlation coefficients for all reported data were >0.99. At least six replicates of each film type were tested for WVP.

Wide-angle X-ray diffraction (XRD)

Wide-angle XRD patterns of film specimens were recorded using Small-Angle X-Ray Scattering (SAXS). This equipment was equipped with a General Area Detector Diffraction System (GADDS) (Bruker AXS, Germany). The area detector operated at a voltage of 40 kV and a current of 45 mA with Cu Kα radiation (λ = 0.15406 nm).

According to the Bragg's equation (1), the gap between MMT-Na^+ layers can be calculated.

$$2d \sin\theta = n\lambda \quad (1)$$

$$n = 1, \lambda = 1.54056\text{Å}$$

This eq. (1) can be applied when the XRD angle is small. Parameter definition is as follows: d is the spacing distance between the diffracting layers, θ is the grazing angle of the incident wave, n is an integer, and λ is the wavelength of the radiation of energy source.

Transmission electron microscopy (TEM)

Ultrathin films (120 nm) for TEM observation were prepared by cutting the nanocomposite sheet at room temperature with Leica ultramicrotome. Thin specimens (120 nm) were collected in a water-filled trough and placed on 200-mesh copper grids. CS/MMT nanocomposite samples were crosslinked in 50% glutaraldehyde before being cut to retard the dissolution of the ultrathin films in the water trough. The TEM images were taken with a Philips Tecnai 12 transmission electron microscope at an accelerating voltage of 120.0 kV and the HRTEM images and SAED patterns were taken with a FEI Tecnai 20 transmission electron microscope equipped with a TVIPS CCD camera at an accelerating voltage of 200.0 kV.

RESULTS AND DISCUSSION

Effect of MMT content

Numerous studies have indicated that the dispersed structure, mechanical properties, and thermal properties vary depending on the clay content.[2,5,13] So, tests were performed to find an appropriate MMT-Na^+ content, in a range of 1–11 % (by weight), capable of enhancing barrier properties and mechanical properties of nanocomposites. The MMT-Na^+ suspension and the chitosan solution were homogenized at 11,000 rpm.

Mechanical properties (tensile strength and elongation at break)

Figure 2 shows tensile strength (TS) and elongation at break (EAB) of CS/MMT nanocomposite films prepared with various MMT-Na^+ contents. The

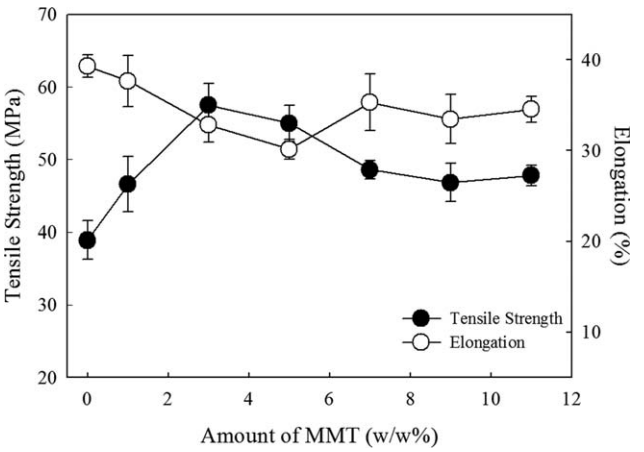

Figure 2 Tensile strength (TS) and elongation at break (%E) of CS/MMT nanocomposite films with different MMT-Na^+ contents.

tensile strength (TS) reached respectively high values of 57.5 and 55.0 MPa at 3% and 5% MMT-Na^+ contents. Addition of higher MMT-Na^+ concentrations (7, 9, and 11 wt %) resulted in decreased TS. In contrast, EAB was lower at 5% MMT-Na^+ than at other concentrations. Other studies showed that clay addition has effectively enhanced the stiffness and tensile strength of the chitosan polymer.[5,12,16] Xu et al.[5] showed that TS of nanocomposite films increased significantly with increasing amount of MMT-Na^+ up to 3%, followed by a decrease with further increase in MMT-Na^+ up to 5%. The results studied by Wang et al.[12] showed that with addition of 2.5% of clay, the moduli of nanocomposites increased by $\sim$ 6.8 %, and that the addition of 10% clay resulted in an increase of about 12%, when comparing to their neat counter parts. Rhim et al.[18] and Koh et al.[19] examined PLA (poly (lactic acid))-based nanocomposite films. The study of Rhim et al.[18] was performed in the range of 0–15% clay contents. The mechanical strength and ductility of the composite films increased at low clay content (2.5%) and decreased with increases in the clay content. Koh et al.[19] studied low level of clay contents (0–0.8%) and showed that tensile strength decreased with increases in organoclay because the brittleness of materials increased.

The improvement in the mechanical properties was believed to be the result of a more uniform dispersion of the clay through the polymer matrix at low concentrations, resulting in an increase in the surface attraction between the clay and the polymer matrix. Earlier optimized concentration, the attractive force between the clay and the polymer matrix was disturbed by the tactoid form of the clay.[5,12,18] The intercalated polymers are regarded as the part of polymer substrate that is physically adsorbed on the surface of silicate and the negatively charged clay acts as an ionic crosslinker. Therefore, the affinity and adsorption with the surface of packing materials made a more effective reduction in the molecular relaxation of the CS matrix.[16,19]

Barrier properties (oxygen permeability and water vapor permeability)

Oxygen permeability (OP) and water vapor permeability (WVP) of CS/MMT nanocomposite films with different MMT-Na^+ contents are presented in Figures 3 and 4, respectively. OP decreased dramatically as the amount of MMT-Na^+ increased up to 5% and it did not change significantly with a little increase above 5% (Fig. 3). Chitosan has a poor barrier property against water vapor because of its hydrophilicity.[15,16] On the other hand, WVP decreased when MMT-Na^+ was increased to 5%, reaching a value of 143×10^{-12} g m/m^2 s Pa. WVP showed a similar tendency to OP and the barrier properties of oxygen and water vapor were improved by increases in MMT-Na up to 5%. According to the research of Koh et al.,[19] improvements in the barrier feature were observed when organoclay contents were increased, through the comparison of gas permeabilities in PLA-based composite film for O_2, N_2, and CO_2. Using PLA-based composite films, Rhim et al.[18] showed that the WVP decreased significantly as the clay content increased.

Low MMT-Na^+ contents resulted in the coexistence of both intercalated and exfoliated structures in the matrix of nanocomposites. With increasing MMT-Na^+ amounts, it was clear that an intercalated morphology with occasional flocculation was present.[12] A tortuous pathway formed by well-dispersed layers of MMT-Na^+ (Fig. 1) acted as a barrier against gas transmission because of the increased path length.[4,18] Since negatively charged clay acts as an ionic crosslinker, the addition of clay will strongly affect the low-swelling ratio as well as the high cross-linking density of chitosan films.[16] The resulting CS/MMT nanocomposite shrunk in the

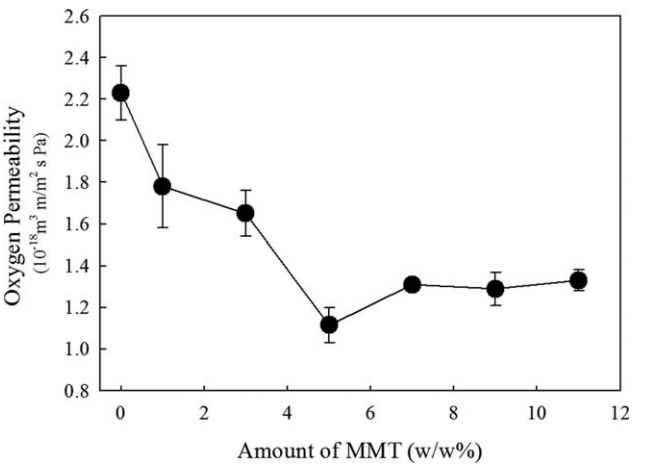

Figure 3 Oxygen permeability (OP) of CS/MMT nanocomposite films with different MMT-Na^+ contents.

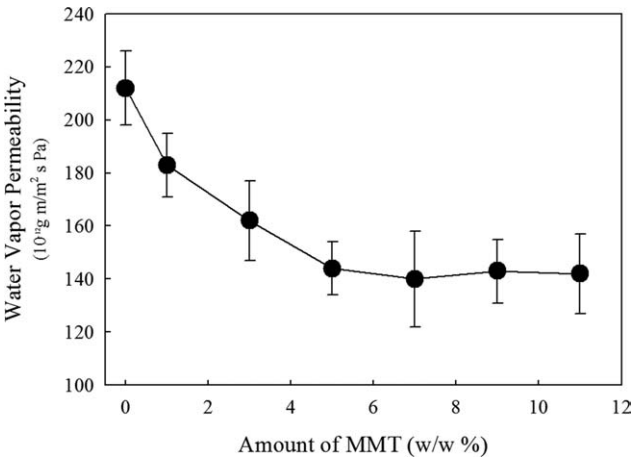

Figure 4 Water vapor permeability (WVP) of CS/MMT nanocomposite films with different MMT-Na^+ contents.

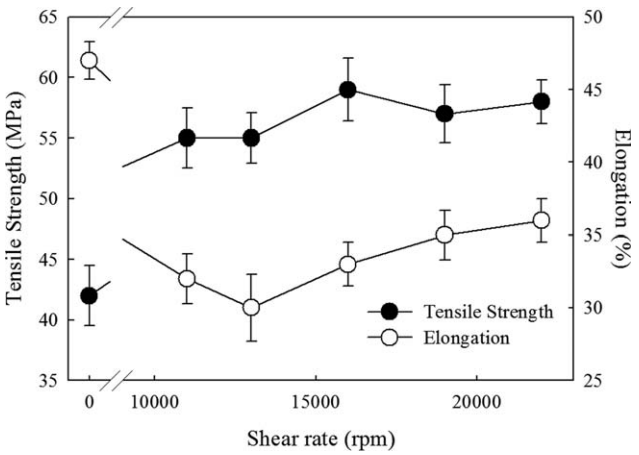

Figure 5 Tensile strength (TS) and elongation at break (EAB) of CS/MMT (5 wt %) nanocomposite films prepared with different shear rates: control was not homogenized.

interlayer space, resulting in pore blocking that inhibited the passage of gas molecules.[2,10] In addition, water vapor was trapped by MMT-Na^+, which have ability to adsorb water because of its thixotropical behavior.[7,11]

Effect of shear rate

When the clay and chitosan are mixed, it is important to form uniformly ordered clay layers into the chitosan polymer matrix. Bousmina[17] announced that rearrangement of MMT-Na^+ layers can be controlled by mechanical stress. Therefore, in this study, homogenization was used to intercalate the chitosan polymer chains into MMT-Na^+ layers. The effect of shear rate on the dispersed structure of MMT-Na^+ layers and the mechanical and barrier properties of CS/MMT nanocomposite films was also investigated. MMT-Na^+ contents of CS/MMT nanocomposite films were fixed at 5% MMT-Na^+.

Mechanical properties (tensile strength and elongation at break)

Figure 5 shows the results of tensile strength (TS) and elongation at break (EAB) determined using CS/MMT nanocomposite films prepared at different shear rates. TS increased with increase in shear rate and the highest value was 59 MPa at 16,000 rpm. It did not change significantly at values higher than 16,000 rpm. EAB of CS/MMT nanocomposite film was lower than the control (0 rpm) but increased above the shear rate of 13,000 rpm.

Barrier properties (oxygen permeability and water vapor permeability)

The effect of shear rate on oxygen permeability (OP) and water vapor permeability (WVP) of CS/MMT nanocomposite films was determined. The lowest value of OP was 4.2×10^{-19} m^3 m/m^2 s Pa and that of WVP was 124 $\times 10$ g m/m^2 s Pa at 16,000 rpm. However, when the shear rate was increased to 16,000 rpm, OP dramatically decreased (Fig. 6). Also, the WVP of the homogenized nanocomposite was lower than the control (0 rpm) but WVP was not significantly affected from shear rate of more than 11,000 rpm (Fig. 7). Therefore, homogenization was effective method for the dispersion of MMT-Na^+ in a chitosan polymer matrix, and the optimal shear rate was 16,000 rpm according to the OP results.

Structural properties

Since one chitosan unit possesses one amino (—NH_2) and two hydroxyl (—OH) functional groups, ion exchange and hydrogen bond take place to form the

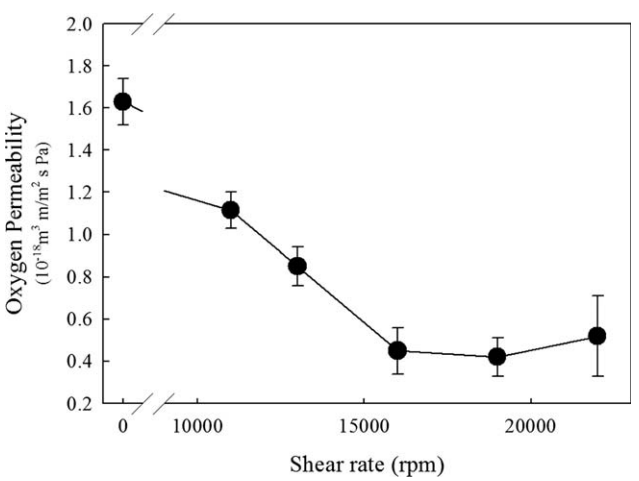

Figure 6 Oxygen permeability (OP) of CS/MMT (5 wt %) nanocomposite films prepared with different shear rates: control was not homogenized.

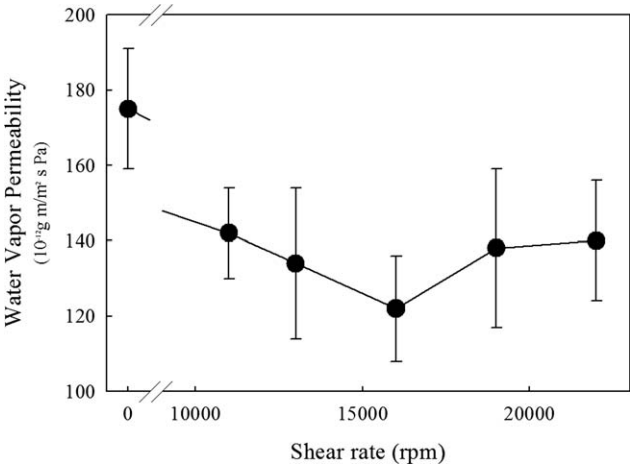

Figure 7 Water vapor permeability (WVP) of CS/MMT (5 wt %) nanocomposite films prepared with different shear rates: control was not homogenized.

CS/MMT nanocomposite film. The positive $-NH_3^+$ groups of chitosan are exchanged for $-Na^+$ in the clay when acidic condition results in conversion of $-NH_2$ groups to $-NH_3^+$.[2,13] This cationic exchange mechanism induces the adsorption process and the role of clay as a crosslinker in the chitosan polymer.[2,9,10,16] Clay contains hydroxylated edge groups and it is believed that they form the flocculated structure of clay in nanocomposites. However, the hydroxyl functional groups can form hydrogen bonds, which lead to the strong interaction between matrix and silicate layers, with two functional groups of chitosan in CS/MMT nanocomposites.[9,12] The direct evidence of the structural type is provided by XRD pattern and TEM image, when the various shear rates were used to form CS/MMT nanocomposite.

Wide-angle X-ray diffraction (XRD). Figure 8 shows XRD patterns of CS/MMT nanocomposite films prepared with different shear rates. The main peak of MMT-Na^+ was observed at $2\theta = 7.3°$ as basal spacing (the (001) plane) and chitosan had small peaks due to crystallization of the polymer. The main peak shifted to a lower reflection angle around $2\theta \approx 4.9°$ and another peak of $2\theta \approx 8.9°$ appeared in the CS/MMT nanocomposite. The peak of $2\theta \approx 4.9°$ indicates that the spacing distance was expanded by Bragg's equation and that MMT-Na^+ layers were dispersed in the chitosan polymer matrix. Wang et al.[12] showed that the d(001) peak observed at $2\theta = 3–5°$ indicates the formation of partly order-intercalated structure. Also, Koh et al.[19] showed that X-ray diffraction patterns, which refer to the specific peak of clay, moved to the lower degree, confirming the formation of an intercalated nanostructure. Another peak of $2\theta \approx 8.9°$ indicated coherent ordering of MMT-Na^+ layers. Sinha Ray et al.[3] explain that the accompanied peak located at a higher degree than original degree was because of aggregation of silicate layers. Also, it was observed that the peaks of $2\theta = 4.8–9.0°$ were smaller and broader than that of MMT-Na^+ indicating the presence of an exfoliated structure of MMT-Na^+ [5]. The coexistence of intercalation, exfoliation, and tactoids was investigated in the CS/MMT nanocomposite through XRD. At 16,000 rpm, the distance of layer was the largest value of 18.87 Å, although this difference was not shown to be significantly different compared with other shear rates. Therefore, the appropriate processing condition for homogenization was 16,000 rpm.

Transmission electron microscope (TEM). TEM is one of the main tools used for determining the nanodispersion of clay layers.[2,5] TEM images of the dispersion of MMT-Na^+ within CS/MMT nanocomposites prepared with different shear rates are presented in Figure 9. MMT-Na^+ layers were not sufficiently dispersed at a shear rate of 0 or 11,000 rpm and were self-aggregated but well ordered at 22,000 rpm. They were well ordered and dispersed in the chitosan polymer matrix at a shear rate of 16,000 rpm compared with other images for samples treated with different shear rates. CS/MMT nanocomposite homogenized at a shear rate of 16,000 rpm was compared with control (0 rpm) in high resolution TEM

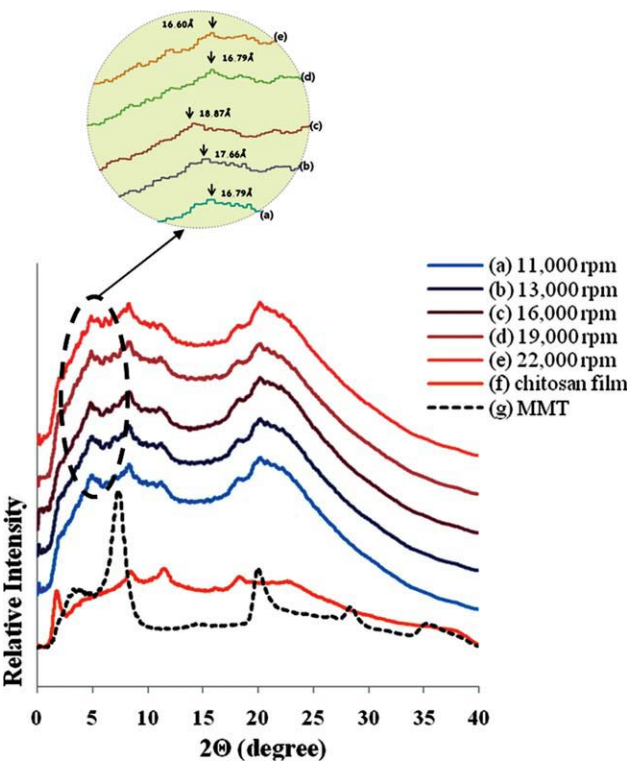

Figure 8 XRD patterns of CS/MMT (5 wt %) nanocomposite films prepared with different shear rates: (a) 11,000 rpm; (b) 13,000 rpm; (c) 16,000 rpm; (d) 19,000 rpm; (e) 22,000 rpm; (f) and (g) are the XRD pattern of chitosan film and MMT-Na^+ powder. [Color figure can be viewed in the online issue, which is available at wileyonlinelibrary.com.]

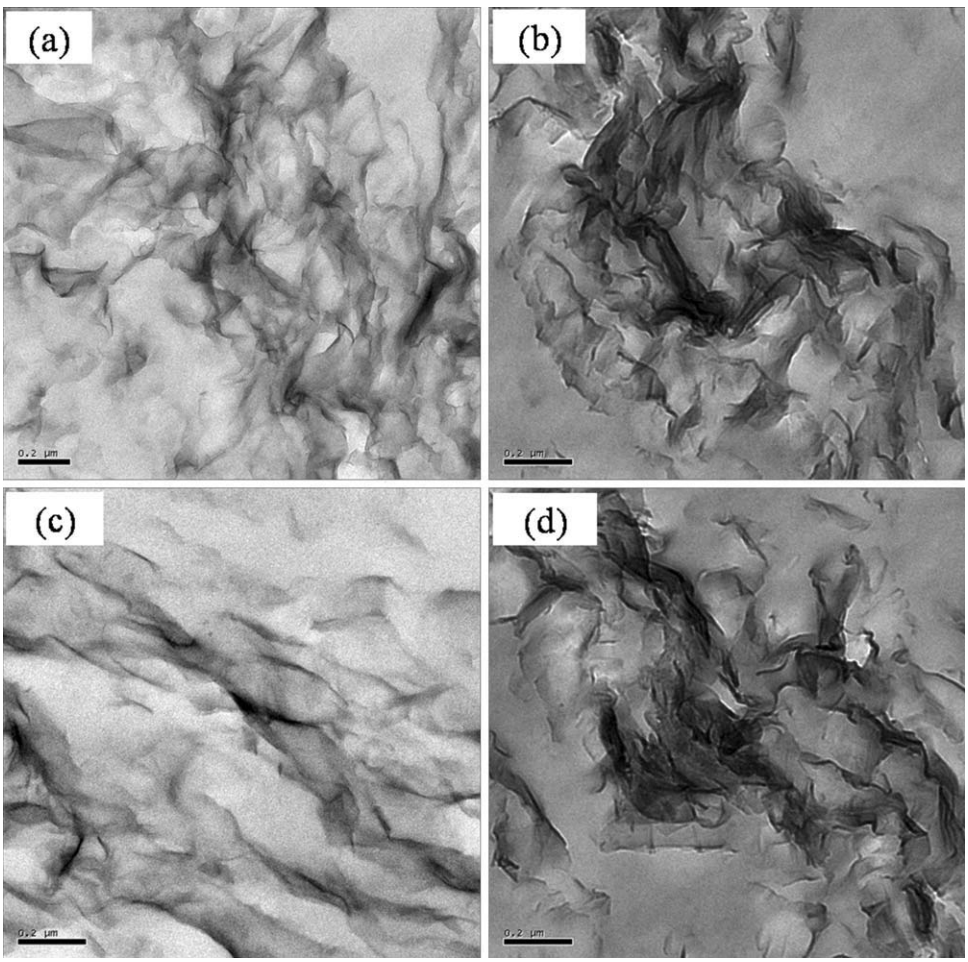

Figure 9 TEM images (low resolution) of CS/MMT nanocomposite films prepared with different shear rates: (a) 0 rpm; (b) 11,000 rpm; (c) 16,000 rpm; and (d) 22,000 rpm.

(Fig. 10). It was confirmed that the gap between MMT-Na^+ layers were expanded and that the chitosan matrices were intercalated into the layers of MMT-Na^+ like Figure 1. Therefore, the optimal shear rate was 16,000 rpm. However, although CS/MMT nanocomposite was generated with these appropriate processing conditions, perfect intercalation was not produced and three dispersion types of MMT-Na^+ layers such as tactoids, exfoliation, and intercalation were investigated as results of XRD.

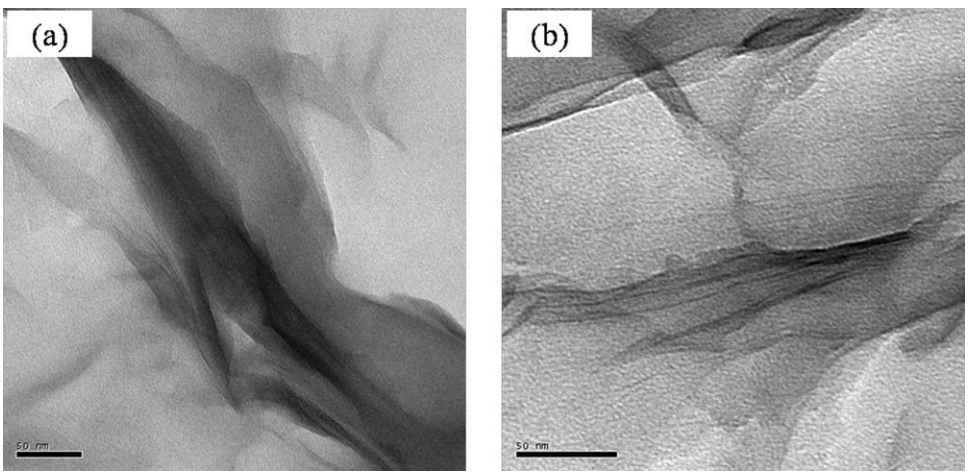

Figure 10 TEM images (high resolution) of CS/MMT nanocomposite films prepared with different shear rates: (a) 0 rpm and (b) 16,000 rpm.

These TEM images were consistent with the results of XRD. Also, it was verified by TEM that the mechanical and barrier properties were not significantly different at greater than 16,000 rpm. Difference in XRD patterns were not obviously observed with changes in shear rate but TEM image of the nanocomposite prepared at 22,000 rpm showed aggregation but parallel arrangement.

CONCLUSIONS

In this study, which was conducted to find appropriate processing conditions for the development of nanocomposites, the samples were prepared using 5% MMT-Na^+, because in terms of mechanical and barrier properties, this was the optimal MMT-Na^+ content. The effect of shear rate during homogenization on the dispersion of MMT-Na^+ in chitosan polymer matrix was studied. EAB increased above the shear rate of 13,000 rpm and the maximum value of TS was obtained at the sample prepared at 16,000 rpm. Also, WVP of the homogenized nanocomposite was lower than that of the untreated nanocomposite but was not significantly altered by shear rate of more than 11,000 rpm. OP decreased with increase in shear rate but was not significantly changed above 16,000 rpm. These results were related to the structure observed by XRD and TEM. TEM images were consistent with the results of XRD, which indicate that three types nanocomposites (tactoids, exfoliation, and intercalation) were generated and the largest distance between MMT-Na^+ layers was produced at 16,000 rpm. These findings were verified by TEM images indicating that the mechanical and barrier properties were not significantly different at more than 16,000 rpm. Difference of XRD pattern with respect to changes in shear rate was not obviously observed. However, TEM images of the nanocomposite prepared at 22,000 rpm showed aggregation but a parallel arrangement. Therefore, homogenization was a beneficial method to disperse effectively MMT-Na^+ layers in a chitosan polymer matrix and a shear rate of 16,000 rpm was optimal for good processing.

References

1. Avella, M.;De Vlieger, J. J.; Emanuela Errico, M.; Fischer, S.; Vacca, P.; Grazia Volpe, M. Food Chem 2005, 93, 467.
2. Darder, M.; Colilla, M.; Ruiz-Hitzky, E. Chem Mater 2003, 15, 3774.
3. Sinha Ray, S.; Maiti, P.; Okamoto, M.; Yamada, K.; Ueda, K. Macromolecules 2002, 35, 3104.
4. Sothornvit, R.; Rhim, J.–W.; Hong, S.-I. J Food Eng 2009, 91, 468.
5. Xu, Y.; Ren, X.; Hanna, M. A. J Appl Polym Sci 2006, 99, 1684.
6. Lin, K.–F.; Hsu, C.–Y.; Huang, T.–S.; Chiu, W.–Y.; Lee, Y.–H.; Young, T.-H. J Appl Polym Sci 2005, 98, 2042.
7. Vaccari, A. Catal Today 1998, 41, 53.
8. Assaad, E.; Azzouz, A.; Nistor, D.; Ursu, A. V.; Sajin, T.; Miron, D. N.; Monette, F.; Niquette, P.; Hausler, R. Appl Clay Sci 2007, 37, 258.
9. Darder, M.; Colilla, M.; Ruiz-Hitzky, E. Appl Clay Sci 2005, 28, 199.
10. Monvisade, P.; Siriphannon, P. Appl Clay Sci 2009, 42, 427.
11. Su, P.–G.; Chen, C.-Y. Sens Actuators B 2008, 129, 380.
12. Wang, S. F.; Shen, L.; Tong, T. J.; Chen, L.; Phang, I. Y.; Lim, P. Q.; Liu, T. X. Polym Degrad Stab 2005, 90, 123.
13. Wang, S.; Chen, L.; Tong, Y. J. Polym Sci Polym Chem 2006, 44, 686.
14. Wang, X.; Chung, Y. S.; Lyoo, W. S.; Min, B. G. Polym Int 2006, 55, 1230.
15. Mao, J.; Zhao, L.; Yao, K.; Shang, Q.; Yang, G.; Cao, Y. J. Biomed Mater Res A 2003, 64, 301.
16. Liu, K.–H.; Liu, T.–Y.; Chen, S.–Y.; Liu, D. M. Acta Biomater 2007, 3, 919.
17. Bousmina, M. Macromolecules 2006, 39, 4259.
18. Rhim, J.–W.; Hong, S.–I.; Ha, C.-S. LWT-Food Sci Technol 2009, 42, 612.
19. Koh, H. C.; Park, J. S.; Jeong, M. A.; Hwang, H. Y.; Hong, Y. T.; Ha, S. Y.; Nam, S. Y. Desalination 2008, 233, 201.